(23)Na multiple-quantum MAS NMR of the perovskites NaNbO(3) and NaTaO(3).

Sharon E. Ashbrook, Laurent Le Pollès, Régis Gautier, Chris J. Pickard, Richard I. Walton

^{23}Na multiple-quantum MAS NMR of the perovskites $NaNbO_3$ and $NaTaO_3$

Sharon E. Ashbrook,†*[a] Laurent Le Pollès,[b] Régis Gautier,[b] Chris J. Pickard‡[c] and Richard I. Walton[d]

Received 28th March 2006, Accepted 9th June 2006
First published as an Advance Article on the web 22nd June 2006
DOI: 10.1039/b604520k

The distorted perovskites $NaTaO_3$ and $NaNbO_3$ have been studied using ^{23}Na multiple-quantum (MQ) MAS NMR. $NaTaO_3$ was prepared by high temperature solid state synthesis and the NMR spectra are consistent with the expected room temperature structure of the material (space group *Pbnm*), with a single crystallographic sodium site. Two samples of $NaNbO_3$ were studied. The first, a commercially available sample which was annealed at 900 °C, showed two crystallographic sodium sites, as expected for the room temperature structure of the material (space group *Pbcm*). The second sample, prepared by a low temperature hydrothermal method, showed the presence of four sodium sites, two of which match the expected room temperature structure and the second pair, another polymorph of the material (space group *P*21*ma*). This is consistent with powder X-ray diffraction data which showed weak extra peaks which can be accounted for by the presence of this second polymorph. Density functional theory (DFT) calculations support our conclusions, and aid assignment of the NMR spectra. Finally, we discuss the measured NMR parameters in relation to other studies of sodium in high coordination sites in the solid state.

Introduction

The use of ^{23}Na NMR for the structural characterisation of the local environment of sodium in the solid state has attracted considerable attention recently for a wide range of chemical systems. Particularly well-studied have been silicate minerals where sodium is found in diverse and often highly unsymmetric coordination environments. Owing to the variety of sodium chemical environments, it can be difficult to relate directly experimental NMR parameters (such as isotropic chemical shift) with coordination geometry (average bond distances and coordination numbers). In addition, ^{23}Na has spin quantum number $I = 3/2$, with spectra broadened by the quadrupolar interaction, even under MAS. This hinders the determination of accurate quadrupole and chemical shift parameters, particularly when a number of crystallographically distinct species are present. However, the development of techniques such as multiple-quantum (MQ) MAS[1] and satellite-transition (ST) MAS,[2] capable of removing completely both first- and second-order quadrupolar broadening, have enabled high-resolution ^{23}Na NMR spectra to be recorded routinely and NMR parameters to be extracted accurately and easily.

Despite the fairly small chemical shift range of ^{23}Na, some general trends with structure have been observed, particularly within groups of similar materials. For example, a number of correlations between isotropic chemical shift (δ_{CS}) and Na–O distances and coordination number,[3–9] have been observed, particularly for silicates[4–6] and fluorides,[8,9] and whilst they are not identical, it is clear that sodium atoms with a larger number of oxygen or fluorine near neighbours (usually, therefore, with a higher average bond distance) exhibit a lower chemical shift. The significant progress in the development of *ab initio* calculations of NMR parameters over the past few years has also facilitated the study of the variation of NMR parameters with structural changes. Many early calculations utilised a cluster approach, ultimately limited in accuracy (and indeed feasibility) by cluster size. Twenty years ago, Schwarz and co-authors showed that the linear augmented plane-wave (LAPW) method was able to predict with high precision electric field gradients in solids.[10] Recent developments of the projector augmented wave formalism (PAW)[11,12] for the calculation of electric field gradients, and its extension, the gauge including projector augmented wave formalism (GIPAW),[13] enabling calculation of both electric field gradients[12] and chemical shielding tensors,[14] now allow accurate calculations to be performed for periodic solids and correlations investigated.[15,16]

In this work we use MQMAS to acquire high-resolution spectra of the oxides $NaNbO_3$ and $NaTaO_3$, and employ density functional theory (DFT) calculations to aid assignment and interpretation of our spectra. The two materials have been characterised structurally by a number of groups and there exists in the literature several reports of

[a] *Department of Earth Sciences, University of Cambridge, Downing Street, Cambridge, UK CB2 3EQ. E-mail: sema@st-andrews.ac.uk; Fax: +44 (0)1334 463808; Tel: +44 (0)1334 463779*
[b] *UMR CNRS 6226 "Sciences Chimiques de Rennes", Ecole Nationale Supérieure de Chimie de Rennes, Campus de Beaulieu, 35700 Rennes, France*
[c] *Cavendish Laboratory, University of Cambridge, J. J. Thomson Avenue, Cambridge, UK CB3 0HE*
[d] *Department of Chemistry, The Open University, Walton Hall, Milton Keynes, UK MK7 6AA*
† Present address: School of Chemistry and EaStCHEM, University of St Andrews, North Haugh, St Andrews, Fife, UK KY16 9ST.
‡ Present address: School of Physics and Astronomy, University of St Andrews, North Haugh, St Andrews, Fife, UK KY16 9SS.

crystallographic studies of each material.[17–23] Both exhibit a rich polymorphism over wide ranges of temperature, but all structures observed are the result of displacive transitions, involving octahedral tilts or rotations within the ideal, cubic ABO_3 perovskite structure. Here, the sodium resides on the (ideally) twelve-coordinate A site, and the Group 5 metal occupies the octahedral B site. At room temperature, $NaNbO_3$ is usually reported to possess an orthorhombic unit cell with a = 5.506 Å, b = 5.566 Å and c = 15.52 Å in space group *Pbcm*[17] (some authors have used the alternative setting *Pbma*) in which two crystallographic sodium sites are found, as in Fig. 1b. A powder neutron diffraction experiment by Darlington and Knight indicated that the symmetry of $NaNbO_3$ at room temperature might be lower than orthorhombic,[21] although another group have subsequently found no evidence for this in a similar study.[23] $NaTaO_3$ has been reported to adopt a structure with an orthorhombic unit cell at room temperature with a = 5.4768 Å, b = 5.5212 Å and c = 7.7890 Å in space group *Pbnm*, but with a smaller volume unit cell than $NaNbO_3$ which includes only one crystallographic sodium site,[22] as in Fig. 1a. Only a few previous ^{23}Na NMR studies of $NaNbO_3$ have been described. For example, an early study by Wolf *et al.*,[24] performed by field sweeping with ν_0 = 10 MHz, was able to determine the presence of two distinct Na sites from the position of singularities in the NMR spectrum, whilst ^{23}Na NMR of $NaNbO_3$ was mentioned, but not shown directly, in the work of Haase *et al.*[25] Aside from the interest in obtaining high-resolution ^{23}Na MQMAS spectra of the two perovskites, where Na has an unusually high coordination number, the complexity of the phase diagrams of $NaNbO_3$ and $NaTaO_3$, with the possible existence of various polymorphs even at room temperature, suggest ^{23}Na NMR may be a useful tool for sample characterisation.

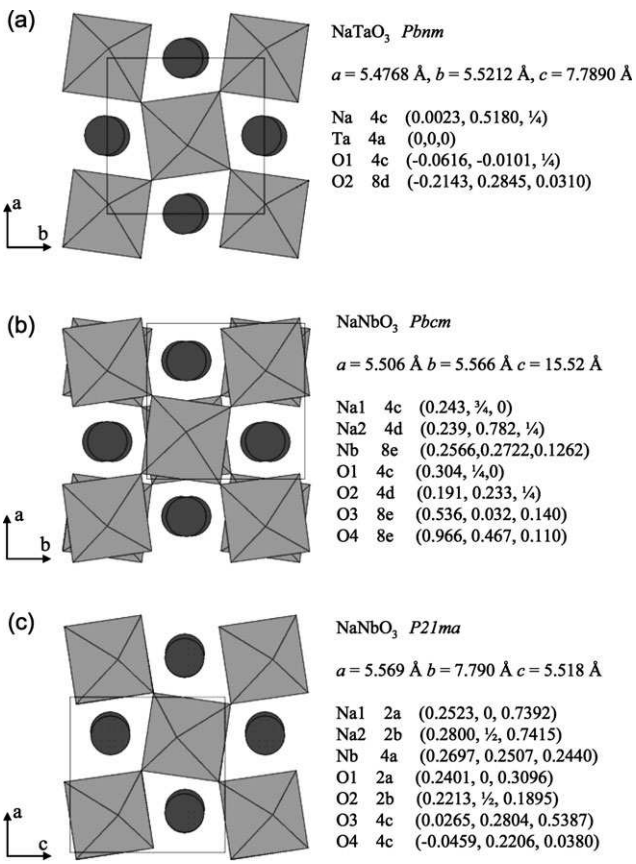

Fig. 1 The structures reported for (a) $NaTaO_3$ and (b, c) $NaNbO_3$. Spheres represent sodium atoms, the octahedra $\{MO_6\}$ units where M = Group 5 metal atom, and the unit cell is represented by the rectangle. Crystallographic data are taken from the literature.[17,22,27]

Experimental

Sample preparation

$NaTaO_3$ was prepared using the method of Kennedy *et al.*:[22] stoichiometric amounts of dry Na_2CO_3 (BDH, 99.9%) and Ta_2O_5 (Aldrich 99%) were finely ground and fired at 700, 800 and 900 °C for 24 h at each temperature with intermittent regrinding, followed by a final firing at 1150 °C. Powder X-ray diffraction (recorded using a Bruker D8 diffractometer operating with Cu Kα radiation, average λ = 1.5418 Å) confirmed that the solid-state reaction was complete and all reflections could be indexed using the 300 K structural model of Kennedy *et al.*[22]

A first sample of $NaNbO_3$ was supplied by Aldrich (100 mesh, no purity stated) and its crystallinity improved by annealing at 900 °C for three days. Powder X-ray diffraction data from this material were consistent with the room temperature structural model deduced by Sakowski-Cowley *et al.*[17] A second sample of $NaNbO_3$ was prepared using a hydrothermal method, based on that of Goh *et al.*:[26] 0.67 g of Nb_2O_5 (Aldrich 99.99%) were stirred into 10 ml of 8.4 M NaOH solution and heated in a 23 ml Teflon-lined, stainless-steel autoclave at 200 °C for 24 h. The white solid was recovered by suction filtration, washed copiously with deionised water and dried at 100 °C in air overnight. Powder X-ray diffraction of the second sample gave data in broad agreement with the expected orthorhombic model of Sakowski-Cowley *et al.*,[17] but weak extra reflections were also observed, as shown in Fig. 2. After searching the Inorganic Crystal Structure Database (ICSD), we discovered that the only possible polymorph of $NaNbO_3$ that matched these extra peaks was one with space group *P*21*ma* reported by Shuvaeva *et al.*,[27] also represented on Fig. 1c. Simulating the powder X-ray pattern as a 50 : 50 mixture of the *Pbcm* and *P*21*ma* polymorphs gave a good fit to the observed powder diffraction data. We will discuss this conclusion further, in the light of the NMR results below.

NMR spectroscopy

^{23}Na MAS NMR spectra were obtained at Larmor frequencies of 52.9, 105.8, 132.2 or 158.7 MHz on Bruker Avance 200, Chemagnetics Infinity 400, Varian Infinity Plus 500 and Bruker Avance 600 spectrometers, respectively. Powdered samples were packed inside either 4-mm or 2.5-mm MAS rotors and rotated at speeds between 10–25 kHz. Spectra are referenced to 1 M NaCl (aq) through a secondary reference of NaCl (s) at 7.3 ppm. Two-dimensional triple-quantum MAS spectra were recorded using the phase-modulated split-t_1 shifted-echo sequence given in Fig. 12a of ref. 28. Typical

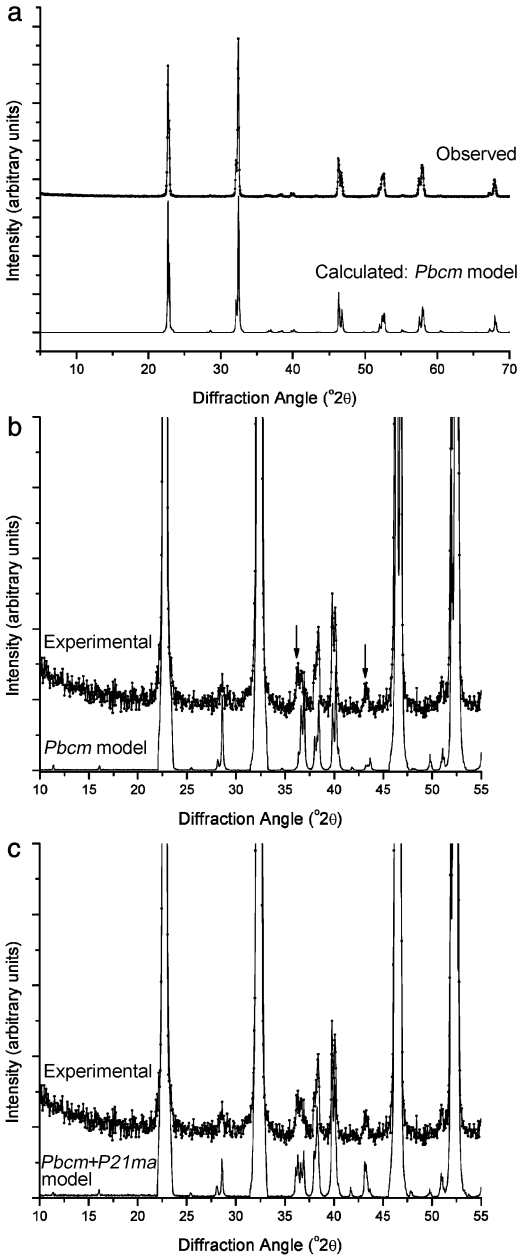

Fig. 2 Powder X-ray diffraction data from hydrothermal $NaNbO_3$ (a) compared to data calculated from the *Pbcm* model, (b) an expanded area with arrows indicating additional intensity not predicted by the *Pbcm* model and (c) compared to data calculated from a model with a mixture of two polymorphs.

radiofrequency field strengths employed were between 80–150 kHz for the triple-quantum excitation and conversion pulses and 10–20 kHz for the final inversion pulse. All spectra were acquired at room temperature ($\sim$18 °C). Any further experimental details may be found in the figure captions.

Calculations

DFT calculations were carried out using the WIEN2k package,[29] and in some cases the NMR-CASTEP code.[30] WIEN2k is a full potential all electron method that utilizes the L/APW + lo approach.[31] The exchange and correlation potentials were calculated using the generalized gradient approximation (GGA) in the parameterization of Perdew–Burke–Ernzerhof.[32] Atomic radii of 1.8, 1.8, 1.4, and 2.5 bohr were used for Nb, Ta, O, and Na spheres, respectively. Charge self-consistency was obtained from 9 and 48 irreducible k points for the calculation of $NaNbO_3$ structures *Pbcm* and *P*21*ma*, respectively. The Brillouin zone integration was performed with 18 irreducible k points for both $NaTaO_3$ structures. The full electric field gradient tensor was calculated from the total self-consistent charge density in the crystal without further approximation. As all electrons are taken into account, the charge redistribution is automatically achieved in the self-consistent field procedure, and thus no additional Sternheimer antishielding factors are required. A ^{23}Na quadrupole moment of 104 mb was employed.[33] As the sign of C_Q is, in most cases, not able to be determined easily directly from a simple MAS spectrum, absolute values of C_Q have been considered.

Both quadrupolar and chemical shift parameters were also calculated using the NMR-CASTEP[30] code, which calculates the chemical shieldings and electric field gradients within periodic boundary conditions and the pseudopotential approximation using the GIPAW[13] and PAW[11–12] methods. Ultrasoft Vanderbilt pseudopotentials were used, with 2s and 2p valence for O, 2s, 2p and 3s valence for Na and 4s, 4p, 5s and 4d valence for Nb. Calculations were performed with a cut-off energy of 689 eV and with 0.05 k points Å^{-3} using GGA (PBE[32]). Geometry optimisations were also performed using this code, with the NMR parameters for the optimised structures then calculated using WIEN2k and/or NMR-CASTEP.

In all calculations (WIEN2k and NMR-CASTEP) a unit cell of the material was considered (8 formula units for $NaNbO_3$ *Pbcm* and 4 formula units for $NaNbO_3$ *P*21*ma*, and both polymorphs of $NaTaO_3$), with the experimental crystallographic parameters (unit cell, atomic positions and space group) as shown in Fig. 1, unless specified.

Results

The ^{23}Na MAS NMR spectra of $NaTaO_3$ recorded at a range of field strengths, B_0, are shown in Fig. 3. All spectra exhibit a single second-order broadened lineshape, with a width (in Hz) proportional to $1/B_0$. The isotropic chemical shift (δ_{CS}) and the quadrupolar coupling, ($C_Q = e^2qQ/h$) and asymmetry (η) may be determined by computer fitting of this lineshape, using the dmfit program,[34] yielding the values given in Table 1. A comparison of the experimental ^{23}Na spectra with those simulated using the fitted parameters is also shown in Fig. 3. (It should be noted that this method of fitting becomes significantly more difficult as the number of crystallographically-distinct species increases owing to overlap of the quadrupolar broadened lineshapes.) Two-dimensional multiple-quantum MAS spectra (shown for B_0 = 9.4 T in Fig. 4) also reveal a single ridge, parallel with the δ_2 axis. The isotropic (or high-resolution) spectrum, obtained from a projection onto δ_1, contains a single, sharp resonance. For MQMAS spectra in general, it is possible to extract information on the quadrupolar and chemical shift interactions from the spectra using a

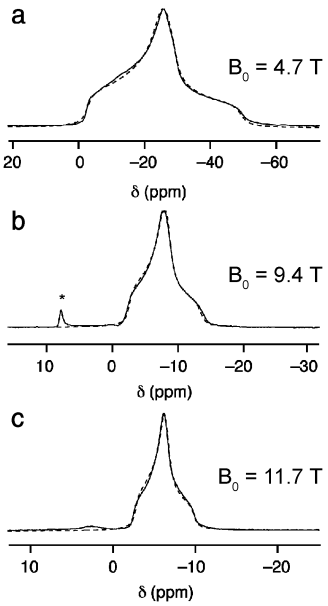

Fig. 3 Experimental ^{23}Na MAS NMR spectra of $NaTaO_3$ and corresponding computer-simulated spectra (denoted by dashed lines) with B_0 of (a) 4.7, (b) 9.4 and (c) 11.7 T. In (a) 480 and (b, c) 240 transients were averaged with recycle intervals of 2 s. The MAS rate was (a) 10, (b) 12 and (c) 16 kHz. Spectra are simulated with C_Q, η, and δ_{CS} of (a) 1.36 MHz, 0.93 and −3 ppm, (b) 1.33 MHz, 0.87 and −2.6 ppm and (c) 1.31 MHz, 0.99 and −2.6 ppm, respectively, derived from computer fitting of the experimental lineshapes. All chemical shifts are shown relative to 1 M NaCl (aq). In (b), a small impurity of NaCl (s) is marked with an asterisk.

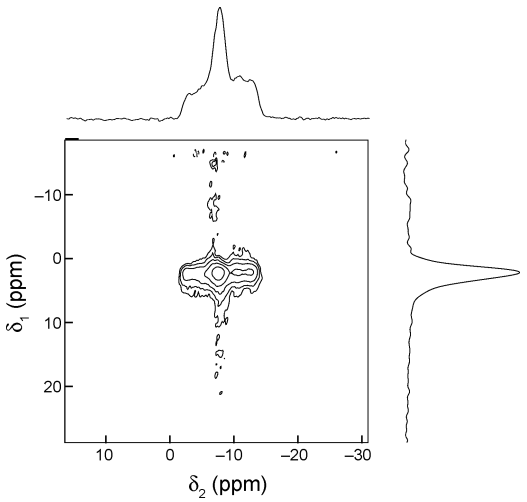

Fig. 4 Two-dimensional ^{23}Na triple-quantum MAS spectrum of $NaTaO_3$, recorded using a phase-modulated split-t_1 shifted echo pulse sequence,[28] with B_0 = 9.4 T. The spectrum is the result of averaging 192 transients with a recycle interval of 2 s, for each of 128 t_1 increments of 50 μs. The MAS rate was 12 kHz. The isotropic projection (onto the δ_1 axis) and cross-section parallel to δ_2 are also shown. All chemical shifts are shown relative to 1 M NaCl (aq).

variety of methods. The position of the centre of gravity of the ridge lineshape (δ_1, δ_2) enables determination of δ_{CS} and P_Q, the quadrupolar product, given by $C_Q\ (1 + \eta^2/3)^{1/2}$. Alternatively, C_Q, η and δ_{CS} may be obtained by computer fitting of a cross-section extracted along the ridge lineshape, parallel to δ_2, in a similar manner to the one-dimensional spectrum, although this lineshape may sometimes be distorted as a result of non-uniform excitation and conversion of triple-quantum coherences, as indeed is the case for the spectrum shown in Fig. 4. Finally, it is also possible to determine δ_{CS} and P_Q from the variation of the δ_1 position of a ridge with B_0 field strength. For example, if δ_1 (in ppm) is plotted against $(1/\nu_0^2)$, where ν_0 is the Larmor frequency in Hz, the result will be (for I = 3/2) a straight line with gradient $(31\ 250P_Q^2)$ and intercept $(17\delta_{CS}/8)$. The values of quadrupolar and chemical shift parameters determined from the MQMAS spectra are also given in Table 1.

Table 1 ^{23}Na NMR parameters for $NaTaO_3$ from the MAS and MQMAS spectra in Fig. 3 and 4

	δ_{CS} (ppm)	C_Q/MHz	η	P_Q/MHz
MAS	−3.0 ± 1.0	1.3 ± 0.1	0.9 ± 0.1	1.5[a]
MQMAS	−2.5 ± 1.0	1.3 ± 0.1	0.95 ± 0.1	1.6 ± 0.1

[a] Calculated from $C_Q(1 + \eta^2/3)^{1/2}$.

The parameters determined from all three field strengths and from different types of spectra are in excellent agreement with each other. The values of the quadrupolar coupling constant and asymmetry are also in good agreement with those calculated by DFT using the WIEN2k package for the room temperature *Pbnm* polymorph, and given in Table 2. However, at all field strengths there are very small discrepancies between the experimental and simulated lineshapes (most noticeable on the exact positions and heights of the distinct shoulders on each lineshape), with the experimental MAS and MQMAS spectra appearing to exhibit a small additional broadening. There are a few possible explanations for such broadening. Perhaps the simplest is that of some extent of distortion within the system. This would produce distributions of both quadrupolar and chemical shift parameters which would additionally broaden the spectra. If such distributions are present they must be fairly small as no significant additional broadening is observed in the two-dimensional MQMAS spectra. An alternative explanation could involve the presence of a higher-order interaction which is unable to be averaged by MAS, such as a second-order quadrupolar–dipolar cross term, arising from dipolar coupling of Na to a nearby quadrupolar ^{181}Ta (I = 7/2) nucleus. Usually such interactions are very small, but the large nuclear quadrupolar

Table 2 Calculated ^{23}Na NMR parameters for $NaTaO_3$ using WIEN2k

Space group	δ_{CS} (ppm)	C_Q/MHz	η	P_Q/MHz
Pbnm (Na1)	—	1.29	0.95	1.48[a]
Cmcm (Na1)	—	1.34	0.44	1.38[a]
Cmcm (Na2)	—	0.63	0.15	0.63[a]

[a] Calculated from $C_Q(1 + \eta^2/3)^{1/2}$.

moment of ^{181}Ta (32 times greater than ^{23}Na) may make this effect small but significant. One final possibility is that the broadening may be due to the presence of a small amount of the high-temperature *Cmcm* phase, undetected by X-ray diffraction. This phase has been reported as existing over the temperature range 723–843 K,[22] but has been found as a minor impurity in samples at room temperature.[35] The ^{23}Na quadrupolar parameters for the two distinct Na species in this phase, calculated by WIEN2k are given in Table 2. It was not possible to detect unambiguously the presence of these resonances in the two-dimensional ^{23}Na spectra, however, although signals with very low intensity (<2% of the maximum and below the contour levels displayed in Fig. 4) were observed.

Fig. 5 shows ^{23}Na conventional MAS and two-dimensional triple-quantum MAS NMR spectra of $NaNbO_3$ (purchased from Aldrich) at field strengths B_0 of 4.7 and 11.7 T. In each case, two distinct resonances, overlapped in the MAS spectrum, are resolved in the MQMAS spectrum. Initial spectra acquired on this sample as purchased exhibited additional broadening as a result of poor crystallinity, but this was improved by annealing the material. The differing widths of the two resonances in Fig. 5 reveal that the two species have very different quadrupolar couplings. This is confirmed in Table 3, which gives the quadrupolar and chemical shift parameters extracted (using the variety of methods described above) from the MAS and MQMAS spectra for the two distinct Na species. This difference in quadrupolar coupling constant (2.1 and 1.0 MHz, respectively, for Na(1) and Na(2)), is responsible for the differing relative intensities observed in the MQMAS spectra. As described previously, the excitation of triple-quantum coherences is non-uniform as the magnitude of the quadrupolar coupling changes. This manifests itself both as lineshape distortions (reflecting the dependence of the quadrupolar interaction upon crystallite orientation) and in non-quantitative signal intensities, as observed in Fig. 5, particularly at the lower B_0 field strength.

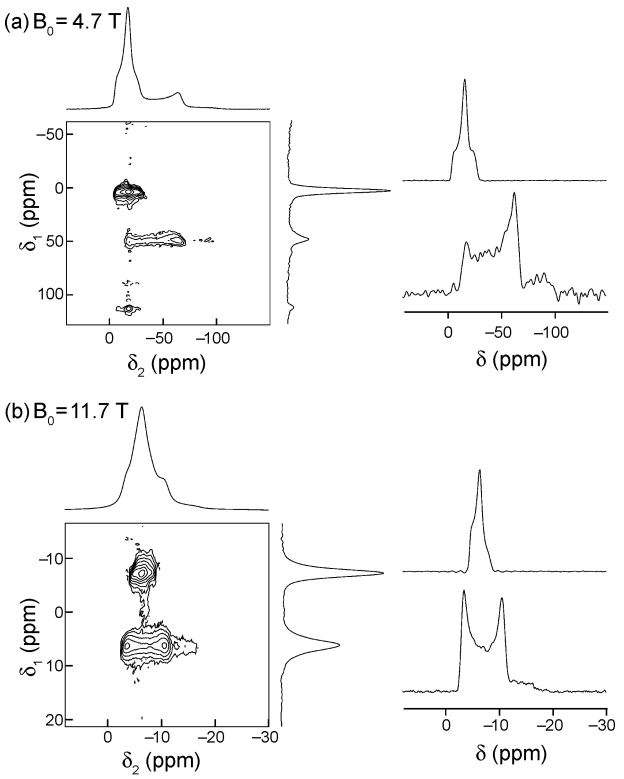

Fig. 5 ^{23}Na MAS NMR of $NaNbO_3$ purchased from Aldrich and annealed at 900 °C. Conventional MAS spectra, two-dimensional triple-quantum MAS (recorded using a phase-modulated split-t_1 shifted echo pulse sequence[28]), corresponding isotropic projections and cross-sections along each ridge lineshape parallel to δ_2 are shown for magnetic field strengths, B_0, of (a) 4.7 and (b) 11.7 T. MAS spectra result from the averaging of (a) 480 and (b) 120 transients with a recycle interval of 2 s. Two-dimensional MQMAS spectra result from the averaging of 192 transients with a recycle interval of 2 s for each of (a) 256 and (b) 160 t_1 increments of (a) 33.3 and (b) 50 μs. The MAS rate was (a) 10 and (b) 20 kHz. All chemical shifts are shown relative to 1 M NaCl (aq).

Table 3 ^{23}Na NMR parameters for $NaNbO_3$ (Aldrich) from the MAS and MQMAS spectra in Fig. 5

	δ_{CS} (ppm)	C_Q/MHz	η	P_Q/MHz
Na(1)	−0.5 ± 1.0	2.1 ± 0.1	0.0 ± 0.1	2.1 ± 0.1
Na(2)	−4.5 ± 1.0	1.0 ± 0.1	0.9 ± 0.2	1.2 ± 0.1

The quadrupolar coupling constants obtained for $NaNbO_3$ are in excellent agreement with those obtained from DFT calculations using WIEN2k (room temperature *Pbcm* polymorph), given in Table 4. However, the agreement of the asymmetry parameter, whilst reasonably good for Na(2), is not in as good agreement for Na(1), where the calculated parameter appears significantly higher than that observed experimentally. This disagreement was also noted in the early work of Wolf *et al.*,[24] where point charge calculations of the Na electric field gradients resulted in good agreement for C_Q, but for Na(1), η ranged between 0.6 and 0.72, in contrast to the experimental value of ~0. Electric field gradient results yielded by NMR-CASTEP (not shown) were in general agreement with those from WIEN2k and also showed a non-zero η for Na(1). However, DFT calculations revealed a force of 2.4 eV Å^{-1} for each Nb atom (much larger than that usually expected ~0.1 eV Å^{-1}), suggesting that its position, as determined by X-ray diffraction, is not optimal. Therefore, a full geometry optimisation was performed (using NMR-CASTEP), allowing the position of all atoms to change, and resulted in a much lower Na(1) η of ~0.01 using WIEN2k, but a increase in the C_Q was also observed (up to 2.5 MHz). Geometry optimisation allowing only the position of the Nb to be altered did not result in any significant change to the Na NMR parameters determined by WIEN2k from those

Table 4 Calculated ^{23}Na NMR parameters for $NaNbO_3$ polymorphs using WIEN2k

Space group	δ_{CS} (ppm)	C_Q/MHz	η	P_Q/MHz
Pbcm (Na1)	—	1.90	0.57	2.00[a]
Pbcm (Na2)	—	0.93	0.75	1.02[a]
*P*21*ma* (Na1)	—	2.03	0.97	2.33[a]
*P*21*ma* (Na2)	—	1.03	0.96	1.18[a]

[a] Calculated from $C_Q(1 + \eta^2/3)^{1/2}$.

obtained initially. These results were also confirmed using NMR-CASTEP. Given the debate in the literature[17–23,27,36] over the exact symmetry of the $NaNbO_3$ structure, perhaps the most likely explanation is a disordering of the Nb position within the NbO_6 octahedra, either time-dependent (dynamic) or static, with only an average value observed by diffraction. Alternatively, the structure may be of a lower symmetry than previously thought. In this respect it should be noted that whilst well-defined ^{23}Na quadrupolar-broadened lineshapes are obtained, ^{93}Nb MAS and MQMAS spectra of $NaNbO_3$ show a distinctly broader lineshape (with $C_Q \approx 20$ MHz) but with few characteristic features of second-order broadening, perhaps confirming the presence of Nb disorder.[37,38] It should also be noted that it is difficult to rule out completely any effects of Na ion motion on the spectra, although these are expected to be small.

Fig. 6 shows similar ^{23}Na MAS and MQMAS spectra (at B_0 field strengths of 4.7, 9.4, 11.7 and 14.1 T) for a sample of $NaNbO_3$ prepared using a hydrothermal method,[26] as described in the experimental section. The MAS spectra look similar to those obtained for the Aldrich sample, although the sharper singularities reflect the better crystallinity of this hydrothermal sample, despite the annealing of the as purchased material. However, significant differences between the two samples are observed in the MQMAS spectra, with additional resonances present in the spectrum of the hydrothermal material. There is significant overlap of spectral resonances and all cannot easily be resolved at a single B_0 field strength. At high B_0, the signal at lower δ_1 appears to be comprised of two closely spaced resonances, whilst that at higher δ_1 ppm, produces a single (albeit broadened) resonance in the isotropic spectrum. Conversely, at low B_0, this resonance is clearly resolved into two distinct peaks, whilst only a single peak is observed at low δ_1. This suggests that the spectrum is composed of four distinct resonances, two with lower C_Q, which are resolved at higher B_0, owing to their differing chemical shifts, and two with much higher C_Q, resolved at lower B_0, as a result of differing second-order quadrupolar shifts. That these latter two resonances are coincident in δ_1 at higher B_0 can also be observed by considering the cross-sections extracted parallel to the δ_2 axis in each spectrum, shown in Fig. 7. The lineshape at 14.1 T (with

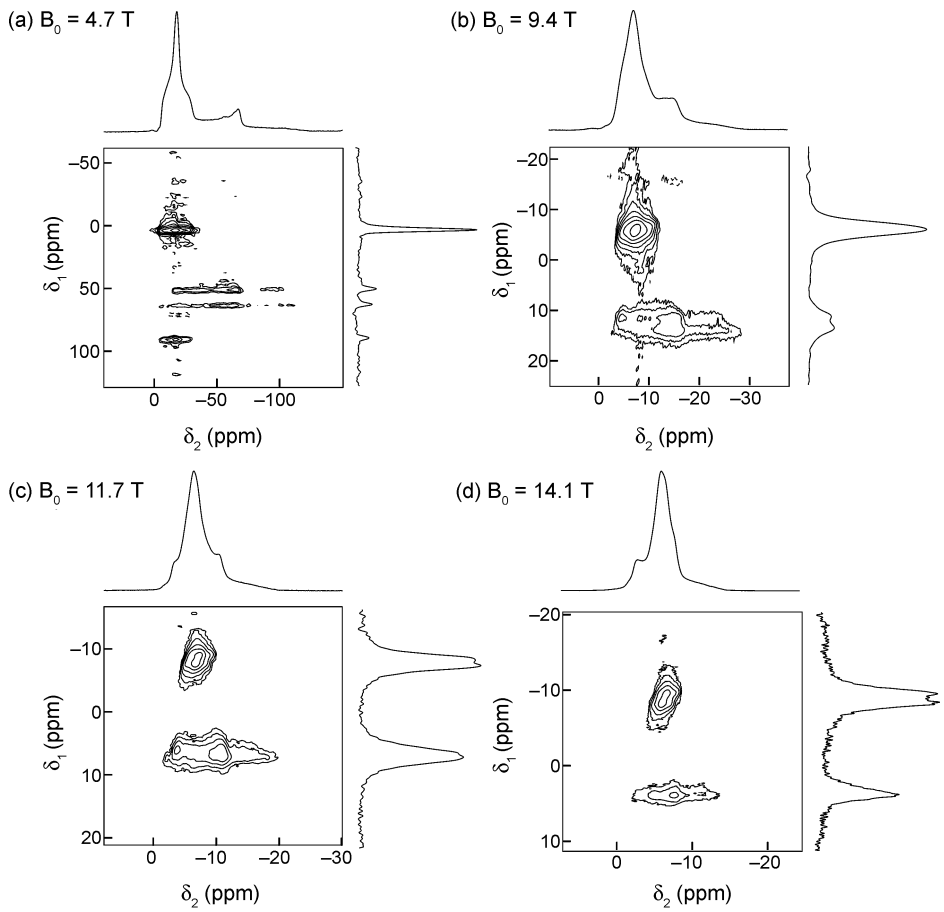

Fig. 6 ^{23}Na MAS NMR of $NaNbO_3$ synthesised by a hydrothermal method. Conventional MAS spectra, two-dimensional triple-quantum MAS (recorded using a phase-modulated split-t_1 shifted echo pulse sequence[28]) and corresponding isotropic projections are shown for magnetic field strengths, B_0, of (a) 4.7, (b) 9.4, (c) 11.7 and (d) 14.1 T. MAS spectra result from the averaging of (a) 480, (b, c, d) 240 transients with a recycle interval of 2 s. Two-dimensional MQMAS spectra result from the averaging of (a) 192, (b) 576, (c) 288 and (d) 192 transients with a recycle interval of 2 s for each of (a) 256, (b) 128, (c) 115 and (d) 192 t_1 increments of (a) 33.3, (b) 50, (c) 110.2 and (d) 148.1 μs. The MAS rate was (a) 8, (b) 12, (c) 16 and (d) 12.5 kHz. All chemical shifts are shown relative to 1 M NaCl (aq).

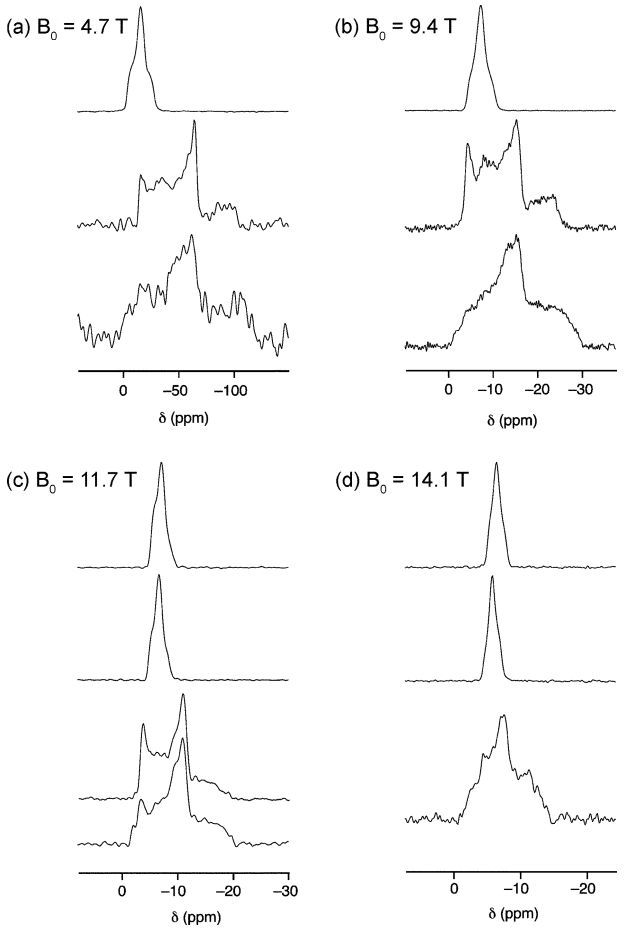

Fig. 7 Cross-sections extracted parallel to the δ_2 axis along the ridge lineshapes in the two-dimensional ^{23}Na triple-quantum MAS NMR spectra of $NaNbO_3$ synthesised by a hydrothermal method, shown in Fig. 6(a)–(d). All chemical shifts are shown relative to 1 M NaCl (aq).

δ_1 = 4 ppm) appears to result from the overlap of two different quadrupolar-broadened powder pattern lineshapes with distinctly different η. Although resolved at low B_0, the lineshapes are then somewhat distorted as a result of non-uniform excitation of triple-quantum coherences, and it is more difficult to extract accurate values for η.

The complexity of these spectra, and particularly the considerable peak overlap, does hinder the extraction of accurate quadrupolar and chemical shift parameters both from the position of the centre of gravity of each lineshape and from cross-sections at particular B_0 field strengths. It should be noted however, that the δ_1 positions of each resonance remain well defined at all field strengths, even when considerable overlap is present. This relationship of δ_1 with B_0 field may be used to determine δ_{CS} and P_Q (as described above). Values for the quadrupole and chemical shift parameters extracted using this approach (and from the centre of gravity or from cross-sections when possible) are given in Table 5 for the four distinct resonances, labelled 1, 2, 3 and 4 in order of increasing δ_1 shift. A comparison of Fig. 5 and 6 and Tables 3 and 5 reveal that resonances 2 and 3 can be clearly identified as Na(2) and Na(1), respectively of $NaNbO_3$ (*Pbcm*), observed in the as purchased sample.

Table 5 ^{23}Na NMR parameters for $NaNbO_3$ (hydrothermal synthesis) from the MAS and MQMAS spectra in Fig. 6 and 7

	δ_{CS} (ppm)	C_Q/MHz	η	P_Q/MHz
1	−5.0 ± 2.0	1.0 ± 0.1	0.7 ± 0.2	1.1 ± 0.1
2	−4.5 ± 2.0	1.0 ± 0.1	0.8 ± 0.2	1.1 ± 0.1
3	−1.0 ± 2.0	2.1 ± 0.1	0.0 ± 0.2	2.2 ± 0.1
4	−1.5 ± 2.0	2.1 ± 0.1	0.9 ± 0.2	2.4 ± 0.1

Peaks labelled 1 to 4 in order of increasing δ_1 shift.

To examine the possibility of additional resonances originating from the *P*21*ma* polymorph, as suggested by the powder diffraction data, we again performed DFT calculations using WIEN2k, the results of which are given in Table 4. The quadrupolar parameters of the two sodiums are very similar to those obtained experimentally, suggesting that our hydrothermal synthesis has indeed resulted in a mixture of the *Pbcm* and *P*21*ma* polymorphs. NMR-CASTEP calculations confirmed the values of these Na electric field gradients and predicted a ~4 ppm difference in the two chemical shifts, as observed experimentally. The relative intensities of the resonances seen in the 4.7 T spectrum suggest that approximately equal amounts of each polymorph are present, consistent with the powder X-ray diffraction data. The NMR parameters are very similar to those obtained for the two resonances in *Pbcm* $NaNbO_3$, resulting in considerable spectral overlap in the MAS spectra, and indeed in the MQMAS spectra at particular field strengths.

It should also be noted that although small differences are observed in the ^{93}Nb MAS spectrum for this material to that for the commercially-available material, the broadened lines observed (as discussed above) prevent the extraction of any detailed information on the number or type of polymorphs present.

Discussion and conclusions

The above results demonstrate the sensitivity of ^{23}Na NMR to local structure and also highlight the need for high-resolution NMR techniques when studying quadrupolar nuclei. Despite very similar MAS spectra, the two samples of $NaNbO_3$ (as purchased and prepared by hydrothermal synthesis) have very different MQMAS spectra, with the presence of two additional resonances in the latter. It should also be noted that full characterisation of these materials required experiments to be performed at more than one B_0 field strength as a result of the differing field dependences of the chemical shift (proportional, in Hz, to B_0) and the second-order quadrupolar interaction (proportional, in Hz, to $1/B_0$), and the similarity of the species present. The fairly large differences in both quadrupolar coupling and chemical shift of the two Na species in the room temperature *Pbnm* $NaNbO_3$, resulting from the distortion or tilting of the NbO_6 octahedra, also emphasizes the sensitivity of NMR to small changes in the local environment.

The ^{23}Na NMR study of the sample of $NaNbO_3$ prepared using hydrothermal synthesis provides independent, complementary evidence to the powder diffraction data that the material contains a mixture of two polymorphs of the

material. In addition to the expected *Pbcm* polymorph we have found convincing evidence that the sample contains a significant proportion of a second polymorph, probably *P*21*ma* (around 50% by mass). The previous report of this polymorph found that the phase was produced in the presence of an electric field, inducing small shifts in the positions of two unique oxide ions, resulting in a structure similar to that of $K_{0.025}Na_{0.975}NbO_3$.[27] It is most likely that it is our use of a low temperature synthetic route (200 °C, instead of in excess of 1000 °C) that has allowed access to this unusual polymorph. It is interesting to note that studies of the synthesis of the perovskite barium titanate, $BaTiO_3$, have shown that a cubic polymorph, usually only seen above 100 °C, may be formed using mild hydrothermal conditions.[39] Previous studies of the hydrothermal synthesis of $NaNbO_3$ used only low-resolution powder X-ray diffraction for phase identification,[26] and so the presence of any weak reflections due to the second polymorph may have been difficult to observe. This demonstrates the power of combining powder diffraction with solid-state NMR (particularly when using calculations to aid spectral assignment) in the characterisation of polycrystalline samples.

As discussed in the Introduction, several authors have noted a general trend of decreasing isotropic chemical shift with increasing average sodium coordination number (and hence average Na–O distance).[3–9] Our newly measured values for sodium $NaTaO_3$ and $NaNbO_3$ fall between 0 and −6 ppm, consistent with this general trend. Despite the fact that sodium is often found in highly irregular coordination environments, Koller *et al.*[5] determined that all oxygen atoms in a sphere with a radius of 3.4 Å around sodium contributed to the observed chemical shift of the sodium and could be considered as part of the immediate coordination environment. Both $NaTaO_3$ and $NaNbO_3$ have structures that are distortions of the ideal, cubic perovskite structure and the nominally twelve-coordinate A site is not a regular cubooctahedron. For $NaTaO_3$, the single crystallographic sodium is surrounded by 12 oxygens at distances ranging from 2.419–3.173 Å, with a mean value of 2.764 Å,[22] whilst for $NaNbO_3$ (*Pbcm*), Na1 has Na–O distances ranging from 2.387–3.129 Å (mean 2.770 Å), and Na2 has Na–O distances ranging from 2.383–3.171 Å (mean 2.777 Å).[17] For the *P*21*ma* polymorph, one sodium has Na–O distances ranging from 2.372–3.148 Å (mean 2.780 Å), and the other, distances ranging from 2.484–3.272 Å (mean 2.784 Å).[27]

Koller *et al.*[5] quantified the relationship between chemical shift and local sodium coordination by considering the bond valence sum of each individual oxygen, W_i,[40] and then introducing a shift parameter, A, for each unique sodium according to the equation:

$$A = \sum_j (W_i / r_i^n) \qquad (1)$$

Here the sum is performed over all cation(j)–oxygen(i) pairs, and n is ideally 3. For the materials studied by Koller *et al.*,[5] the majority of which were silicates and phosphates, a linear relationship between isotropic chemical shift and A was observed. We have found that for $NaTaO_3$ and $NaNbO_3$, the measured values of chemical shift do not fit this correlation, and in fact much more negative chemical shifts would be expected if the correlation was extrapolated to the A values for sodium in these perovskite materials. For example, for $NaTaO_3$, A for the unique sodium is 1.28, giving an expected isotropic chemical shift of −55.6 ppm (correcting the chemical shift to be referenced to NaCl (s) at 7.3 ppm as in our measured data). The only transition-metal oxide material that Koller *et al.* studied was $NaCr_2O_4$, which contains two unique sodiums, one of which has ten oxygen neighbours at less than 3.4 Å, at an average distance of 2.86 Å (note this is a longer average distance than for the 12 coordinate sodium ions found in the perovskite materials) and was observed to have an isotropic chemical shift of −12.2 ppm. In a separate work, Xue and Stebbins[4] studied a series of silicates and noted that a correlation of the chemical shift with the average Na–O interatomic distance is often more applicable than the correlation of Koller *et al.* It was noted in this work that in many simple systems the determination of coordination number (required for the bond valence analysis) is usually unambiguous, but that for ternary systems the often continuous distribution of distances observed makes this determination somewhat arbitrary.

It has also been shown that the chemical shift range associated with a particular coordination number and atom can be fairly large (for example, Na coordinated by six O atoms is given by Koller *et al.*[5] as ranging from −20 to +10 ppm in the materials studied). This is attributed to the dependence of the chemical shift upon the particular chemical environment of the coordinating atoms themselves, *i.e.*, the elements to which they themselves are bonded. It is noticeable that when the surrounding oxygens are bonded to less electronegative elements the chemical shift is in general more positive. Despite the large coordination number of Na in the perovskite materials, the electronegativities of Nb and Ta are reasonably low, perhaps therefore resulting in a more positive chemical shift. This demonstrates how any correlation between chemical shift and structural parameter is dependant on the detail of the number and type of coordinating atom and also on the more longer range structural features. The chemical nature of the solid as a whole strongly affects the chemical shift and it appears that next-nearest neighbour interactions must also be considered in the heavier transition-metal oxides we have studied.

Only a few other materials with high (>8) sodium coordination number have been studied using ^{23}Na MAS NMR. These include the minerals nepheline (−5.5 and −19.5 ppm for 8 and 9 coordinate sodium, respectively), microcline (−24.3 ppm for 9 coordinate Na) and tourmaline (−13 ppm for 9 coordinate Na) and the material $Na_2LiYSi_6O_{15}$ (−18 ppm for 9 coordinate Na).[7] Fluorine containing materials studied include the perovskite $NaBaLiNiF_6$ (for which a Na chemical shift of ~0 ppm may be inferred from the spectra presented,[41] and the alkali fluorites cryolite, Na_3AlF_6, (2.4 and −9.3 ppm for 6 and 8 coordinate sodium)[9,42] and chiolite, $Na_5Al_5F_{14}$, (−6 and −21 ppm for 6 and 8 coordinate sodium).[9] In all cases, the general trend that larger numbers of more distant coordinating atoms results in a decrease in chemical shift was apparent, but that detailed correlations of shift with structural parameters is far from trivial. It should be noted that many other A-site sodium perovskites contain paramagnetic metal

ions, for example the tungsten bronzes Na_xWO_3, the U(IV) material $NaUO_3$, and the fluorides $NaMF_3$ (M = V, Mn, Co), so measurement of ^{23}Na MAS NMR spectra is not straightforward.

In conclusion, we have used ^{23}Na MAS NMR, in conjunction with DFT calculations to aid spectral interpretation, for the study of two perovskite materials, $NaTaO_3$ and $NaNbO_3$, where Na is found in an unusually high coordination number environment. The high-resolution achieved by MQMAS was able to determine that our as synthesised sample contained a probable mixture of two polymorphs of $NaNbO_3$, namely *Pbcm* and *P*21*ma*. The isotropic chemical shifts we extracted from the two-dimensional spectra were small, in agreement with many literature observations that the chemical shift tends to decrease when Na is coordinated by a larger number of atoms at greater distances. However, a search of the literature provides evidence that detailed correlation with structural parameters is difficult and more long range effects must be taken into account.

Acknowledgements

We thank Dr Stephen Wimperis and Professor Christian Jäger for the use of Bruker Avance spectrometers in Exeter (4.7 T) and Berlin (14.1 T), respectively. SEA thanks the Royal Society for the award of a Dorothy Hodgkin Research Fellowship. LLP and RG thank the Institut de Développement et de Ressources en Informatique Scientifique (IDRIS-CNRS) and the Centre Informatique National de l'Enseignement Supérieur (CINES) for the use of their computing facilities. CJP is supported by an EPSRC Advanced Research Fellowship.

References

1 L. Frydman and J. S. Harwood, *J. Am. Chem. Soc.*, 1995, **117**, 5367.
2 Z. Gan, *J. Am. Chem. Soc.*, 2000, **122**, 3242.
3 S. Antonijevic, S. E. Ashbrook, R. I. Walton and S. Wimperis, *J. Mater. Chem.*, 2002, **12**, 1469.
4 X. Xue and J. F. Stebbins, *Phys. Chem. Miner.*, 1993, **20**, 297.
5 H. Koller, G. Engelhardt, A. P. M. Kentgens and J. Sauer, *J. Phys. Chem.*, 1994, **98**, 1544.
6 A. M. George and J. F. Stebbins, *Am. Mineral.*, 1995, **80**, 878.
7 H. Maekawa, T. Nakao, S. Shimokawa and T. Yokokawa, *Phys. Chem. Miner.*, 1997, **24**, 53.
8 J. F. Stebbins, I. Farnan, N. Dando and S. Y. Tzeng, *J. Am. Ceram. Soc.*, 1992, **75**, 3001.
9 P. J. Dirken, J. B. H. Jansen and R. D. Schuiling, *Am. Mineral.*, 1992, **77**, 718.
10 P. Blaha, K. H. Schwarz and P. Herzig, *Phys. Rev. Lett.*, 1985, **54**, 1192.
11 H. M. Petrilli, P. E. Blöchl, P. Blaha and K. Schwarz, *Phys. Rev. B*, 1998, **57**, 14690.
12 M. Profeta, F. Mauri and C. J. Pickard, *J. Am. Chem. Soc.*, 2003, **125**, 1–541.
13 C. J. Pickard and F. Mauri, *Phys. Rev. B*, 2001, **63**, 245101.
14 J. Yates, PhD thesis, University of Cambridge, 2003.
15 G. Silly, C. Legein, J. Y. Buzare and F. Calvayrac, *Solid State Nucl. Magn. Reson.*, 2004, **25**, 241.
16 T. Charpentier, S. Ispas, M. Profeta, F. Mauri and C. J. Pickard, *J. Phys. Chem. B*, 2004, **108**, 4147.
17 A. C. Sakowski-Cowley, K. Lukaszewicz and H. D. Megaw, *Acta Crystallogr., Sect. B*, 1969, **25**, 851.
18 H. D. Megaw and C. N. W. Darlington, *Acta Crystallogr., Sect. B*, 1973, **29**, 2171.
19 M. Ahtee and C. N. W. Darlington, *Acta Crystallogr., Sect. B*, 1980, **36**, 1007.
20 C. N. W. Darlington and K. S. Knight, *Acta Crystallogr., Sect. B*, 1999, **55**, 24.
21 C. N. W. Darlington and K. S. Knight, *Physica B*, 1999, **266**, 368.
22 B. J. Kennedy, A. K. Prodjosantoso and C. J. Howard, *J. Phys.: Condens. Matter*, 1999, **11**, 6319.
23 H. Xu, Y. Su, M. L. Balmer and A. Navrotsky, *Chem. Mater.*, 2003, **15**, 1872.
24 F. Wolf, D. Kline and H. S. Story, *J. Chem. Phys.*, 1970, **53**, 3538.
25 J. Haase, M. S. Conradi and E. Oldfield, *J. Magn. Reson.*, 1994, **109**, 210.
26 G. K. L. Goh, F. L. Lange, S. M. Haille and C. G. Levi, *J. Mater. Res.*, 2003, **18**, 338.
27 V. A. Shuvaeva, M. Y. Antipin, S. V. Lindeman, O. E. Fesenko, V. G. Smotrakov and Y. T. Struckov, *Kristallografiya*, 1992, **37**, 1502.
28 S. P. Brown and S. Wimperis, *J. Magn. Reson.*, 1997, **128**, 42.
29 P. Blaha, K. Schwarz, G. K. H. Madsen, D. Kvasnicka, J. Luitz, *Computer Code WIEN2k*, Vienna University of Technology, Austria, 2001, ISBN 3-9501031-1-2.
30 M. D. Segall, P. J. D. Lindan, M. J. Probert, C. J. Pickard, P. J. Hasnip, S. J. Clark and M. C. Payne, *J. Phys.: Condens. Matter*, 2002, **14**, 2717.
31 G. K. H. Madsen, P. Blaha, K. Schwarz, E. Sjöstedt and L. Nordström, *Phys. Rev. B*, 2001, **64**, 195134.
32 J. P. Perdew, K. Burke and M. Ernzerhof, *Phys. Rev. Lett.*, 1996, **77**, 3865.
33 P. Pyykkö, *Mol. Phys.*, 2001, **99**, 1617.
34 D. Massiot, F. Fayon, M. Capron, I. King, S. Le Calve, B. Alonso, J. O. Durand, B. Bujoli, Z. Gan and G. Hoatson, *Magn. Reson. Chem.*, 2002, **40**, 70.
35 K. S. Knight, personal communication.
36 Y. I. Yuzyuk, P. Simon, E. Gagarina, L. Hennet, D. Thiaudière, V. I. Torgashev, S. I. Raevskaya, I. P. Raevskii, L. A. Reznitchenko and J. L. Sauvajol, *J. Phys.: Condens. Matter*, 2005, **17**, 4977.
37 S. Prasad, P. Zhao, J. Huang, J. J. Fitzgerald and J. S. Shore, *Solid State Nucl. Magn. Reson.*, 2001, **19**, 45.
38 S. E. Ashbrook and S. Wimperis, *J. Magn. Reson.*, 2002, **156**, 269.
39 P. K. Dutta and J. R. Gregg, *Chem. Mater.*, 1992, **4**, 843.
40 I. D. Brown and D. Altermatt, *Acta Crystallogr., Sect. B*, 1985, **41**, 244.
41 M. Ducau, K. S. Suh, J. Senegas and J. Darriet, *Mater. Res. Bull.*, 1992, **27**, 1115.
42 M. Kotecha, S. Chaudhuri, C. P. Grey and L. Frydman, *J. Am. Chem. Soc.*, 2005, **127**, 16701.